

Time-Resolved Infrared Spectroscopy as an In Situ Tool To Study the Kinetics During Self-Assembly of Mesostructured Films

Plinio Innocenzi* and Tongjit Kidchob

Dipartimento di Architettura e Pianificazione, Laboratorio di Scienza dei Materiali e Nanotecnologie, Università di Sassari, Nanoworld Institute, Palazzo del Pou Salid, Piazza Duomo 6, 07041 Alghero (Sassari), Italy

Johnny Mio Bertolo

IMM-CNR Sez. di Roma, Area di Ricerca di Roma "Tor Vergata", 00133 Rome, Italy

Massimo Piccinini,[†] Mariangela Cestelli Guidi, and Claudio Marcelli

Laboratori Nazionali di Frascati—INFN, Via E. Fermi 40, 00044 Frascati, Italy

Received: January 5, 2006; In Final Form: April 5, 2006

Rapid scan time-resolved infrared spectroscopy has been used to investigate in situ the kinetics of the chemical processes involved in the formation of self-assembled mesostructured films. The experiments have been done in transmission mode on films cast on a diamond disk using an infrared microscope. Two specific materials have been studied: silica and titania mesoporous films templated by a triblock copolymer surfactant (Pluronic F-127). The time dependence of solvent evaporation and condensation of the chemical species have been clearly observed. Different stages in the film formation have been identified, which support well the general theory of self-assembly. The in situ FTIR spectroscopy using time-resolved rapid scan has proven to be a very effective tool for in situ analysis of film formation from a liquid phase.

Introduction

The process of organization of self-assembled porous meso-organized materials is driven by solvent evaporation,¹ but several chemical reactions have to follow the right kinetics in order to achieve organization.² In particular, self-assembly becomes a critical process during the preparation of thin films, when solvent evaporation is very fast and the critical micelle concentration is reached during the deposition.³

Mesostructured porous films are deposited using precursor solutions containing an alkoxide (or an organically modified alkoxide) or a metal chloride or mixtures of both, the supramolecular template (the most common are ionic or block-copolymers) and alcohols or ethers as solvents. The precursor sol is maintained in very high acidic conditions to avoid condensation of the precursors that tend to form aggregates through sol–gel reactions, if not adequately controlled. In these conditions, the precursors are highly hydrolyzed but not condensed; polycondensation is achieved only with the increase of pH due to the evaporation of the solvent and part of the acid with it.

Basically, three processes are simultaneously induced by solvent evaporation during self-assembly: the formation and organization of the templating micelles; the formation of “nanobricks” through the sol–gel polycondensation reactions; the consequent formation of an interface between the micelles and the “nanobricks”. To achieve an organized structure, the kinetic constants involved in the process have to follow the following hierarchy:⁴

$$k_{\text{inter}} > k_{\text{org}} > k_{\text{inorg}} \quad (1)$$

where k_{inter} , k_{org} , and k_{inorg} are the relative rates for interface formation, organic template array assembly, and inorganic polycondensation, respectively.

Different in situ techniques have been developed and applied to obtain direct scientific evidence of the self-assembly process. In situ small-angle X-ray scattering (SAXS), in particular, has allowed us to clarify several of the parameters that are controlling the formation of organized porous phases.⁵ In situ SAXS is highly informative but can give direct evidence only about the formation in real time of organized structures.⁶ The simultaneous kinetics of solvent evaporation and polycondensation, which are the processes that indeed drive self-assembly, cannot be observed. Other techniques have been combined with SAXS in situ, such as optical interferometry,⁷ to characterize the evaporation induced self-assembly process.⁸

Examples of applications of FTIR spectroscopy for studying in situ film formation have been reported by Doshi⁹ et al. and by the present authors.¹⁰ In the experiment reported by Doshi, infrared spectra of cast films were recorded in situ by attenuated total reflectance Fourier infrared (ATR-FTIR) spectroscopy. The time scale that was used (the spectra were recorded every 14 s) did not allow us, however, to observe the true kinetics of the process. A different configuration was used by our group that performed an in situ FTIR experiment in transmission on self-assembling cast films of silica and organically modified hybrid silica.¹⁰ The experimental setup allowed us to decrease the time scale to 1 s to reach a better insight into the process.

In the present article, we introduce a new approach based on the application of time-resolved FTIR spectroscopy to enlighten the kinetics and the processes behind the deposition of self-assembled mesoporous films. We have applied this method to

*Corresponding author. E-mail: plinio@uniss.it. Fax: +39-079-9720420.

[†] Also at Dipartimento di Scienze Geologiche, Università Roma Tre, Largo S. Leonardo Murialdo, 1-00146 Rome, Italy.

mesoporous materials, but the technique can have a more general application to films deposited from a liquid phase. We have used rapid scan time-resolved (RSTR) measurements that allow the acquisition of spectra in quick succession. Typically, time-resolved measurements are performed to record sample changes or environmental fluctuations, to achieve absolute time resolution (i.e., maximum possible number of measurements) or to repeat measurements with a high time constant. The experimental setup, that we have developed, can be generally used to study different types of films prepared from a liquid phase. This is also, to our knowledge, the first application of time-resolved infrared spectroscopy to the study in situ liquid film deposition.

Experimental Section

Silica sols were prepared using tetraethyl orthosilicate (TEOS), H₂O, ethanol (EtOH), HCl, and a triblock copolymer (Pluronic F127) as templating agent, with the following final molar ratios of reagents: TEOS:EtOH:H₂O:HCl:F127 = 1:24.48:14.70:0.11:7.6 × 10⁻³. To prepare the precursor silica sol, we prepared a stock solution by adding EtOH, TEOS, water, and HCl in this order in the following molar ratios: TEOS:EtOH:H₂O:HCl = 1:2.78:1.04:56.2 × 10⁻³. The sol was left to react for 1 h under stirring at room temperature. A second solution was prepared by dissolving 1.3 g of Pluronic F-127 in 15 cm³ of EtOH and 1.5 cm³ of acid aqueous solution (0.05 M HCl). The final sol was obtained by adding 7.7 cm³ of the stock sol to the solution containing the block copolymer. The final solution was reacted for 24 h under stirring, and then, it was aged at 28 °C for 1 week.

Titania sols were prepared using TiCl₄, EtOH, H₂O, and Pluronic F127, with the following molar ratios: TiCl₄:EtOH:F127:H₂O = 1:40:0.005:10. The precursor sol was obtained by slow addition of TiCl₄ into a mixture of EtOH and surfactant; water was added, drop by drop, after 5 min of stirring.

Time-resolved in situ infrared (IR) analysis was performed at the synchrotron infrared beamline (SINBAD) at the Laboratori Nazionali (Frascati, Italy) of the Istituto Nazionale di Fisica Nucleare (INFN) using a Bruker equinox 55 modified to work down to 10⁻² mbar; a conventional Globar source was used. The IR measurements were performed using the interferometer working in a vacuum, in the range 500–6000 cm⁻¹ and with a resolution of 8 cm⁻¹. An MCT detector (1 mm² size) cooled to the nitrogen temperature and a KBr beam splitter were used. Rapid scan time-resolved measurements were performed by a single scan per spectrum and an acquisition time of 133 ms followed by an interval of 160 ms before the beginning of the new measurement. A small drop of a controlled amount of the precursor sol (2–5 μL) was cast on the diamond disk, and immediately afterwards the measurement was started.

The percent relative humidity (RH %) during the experiment was carefully monitored, and a special room was built around the microscope in order to control the RH. RH values for silica and titania sols were maintained lower than 40% and 30%, respectively.

The experiments were done in transmission configuration with a Bruker IR microscope that was installed laterally with respect to the interferometer. A diamond disk was selected as substrate because of the excellent transmission in the 700–2000 cm⁻¹ region.¹¹ The background was recorded in air with the diamond disk.

In a typical experiment, a small drop of precursor solution was cast on the diamond disk, and immediately afterwards, the IR spectra were recorded in transmission by RSTR spectroscopy in order to follow the evaporation and condensation processes

involved in the film formation; the results are plotted as 3D spectra (Bruker Opus 5.5 software).

Results and Discussion

Data Analysis and Sources of Errors. The choice of the experimental conditions, to perform FTIR in situ experiments during the deposition of films from liquid phase, is particularly critical, because of the signal saturation and the process time scale. We have carefully selected the volume of the sol drop to be cast to get better reproducibility of the experiment and to avoid saturation of the signal. The intensities of the vibrational modes due to ethanol and water, especially at the first stage of the deposition process, are very intense and can easily saturate the detector. The selection of the sol drop volume is therefore a critical issue, also because the evaporation rate is highly dependent on the sol volume; in smaller drops the evaporation is much faster. Several runs of the same experiments have been performed to test the reproducibility of the technique.

We have selected the rapid scan time-resolved FTIR analysis instead of step scan because this method allowed us to reach a good compromise in terms of signal-to-noise ratio and acquisition time rate.¹² The kinetics of the process do not evolve, in fact, over a very short time scale to require a step scan analysis, and we have used the RSTR method recording one spectrum in 133 ms.

Application of time-resolved IR spectroscopy to a kinetic process, such as film deposition from a liquid phase, requires also a careful treatment and evaluation of the data. The film thickness, in fact, decreases with the time, as the evaporation of the solvent proceeds. This time-dependent change of film thickness induces a different light scattering from the sample and a shift of the baseline. Some “ghost” processes can appear, in this case, without a specific treatment of the single spectra recorded by RSTR infrared spectroscopy. We have extracted the spectra from the sequential 3D-RSTR file and introduced the baseline correction by a concave rubberband correction method (OPUS 5.5 software) using 64 baseline points and 20 iterations.

Another problem in performing FTIR in situ experiments during the deposition of films from liquid phase is the high overlapping of the vibrational modes of the different chemical species involved in the process. Understanding of the kinetics and the reactions needs separation of the different signals, in terms of resolution and intensity, which is very difficult to obtain. The formation of the silica walls, for instance, can be observed by the appearance of the Si–O–Si stretching modes (ν_{as} , 1070 cm⁻¹), which is, however, overlapped with signals from ethanol, TEOS, and the surfactant (see, for reference, the spectra reported in Supporting Information). In these conditions it is almost impossible to extract information about kinetics and reactions during a film deposition with conventional FTIR measures. Deconvolution methods are unreliable because of the many overlapped signals.¹³ This problem has, therefore, not allowed an effective application of in situ FTIR during deposition of films from liquid phases in which solvent evaporation and polycondensation are involved. Three-dimensional spectra recorded by RSTR measurements give a possible alternative for visualizing the process in a simple and effective way. Of course, no direct information can be obtained about organization of the structure, and separate in situ experiments have to be performed by SAXS.^{14,15}

Silica Films. There are three main processes that can be monitored by in situ FTIR time-resolved experiments: ethanol and water evaporation and oxide polycondensation. We have

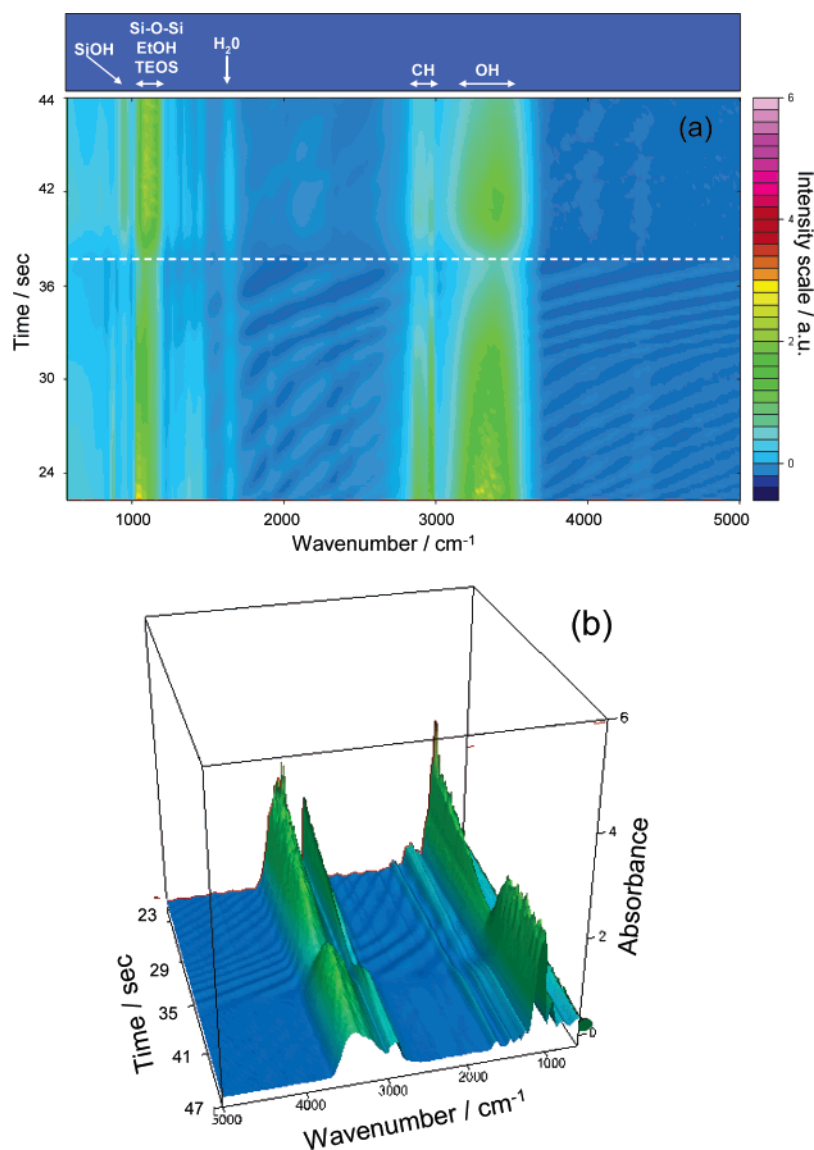


Figure 1. Three-dimensional FTIR images (a and b) obtained during the deposition by casting of a self-assembling silica film. The images are recorded by rapid scan time-resolved method.

used as a case study silica and titania films because these are the two more studied self-assembled mesoporous systems, and several in situ data are also available from other techniques.^{9,16} A comparison with these data can allow evaluation of the reliability of the RSTR method.

The results of the RSTR measurements during casting of a silica film (with Pluronic F127 as templating agent) are shown in Figure 1. Figure 1 is a 3D representation of the RSTR measurements, with the wavenumber and the time in the *x*- and *y*-axes, respectively, and the intensity changes in a color scale. At the first stage of film formation, the solvent evaporation is the predominant process, and the ethanol signature (1044, 1095, and ~ 1400 cm^{-1}) saturates a great part of the other vibrational modes. The film is rich in water and ethanol, and the condensation process is not yet started. The end of this process is clearly recorded by RSTR; in fact, a discontinuity in the 3D spectra (Figure 1a,b) is observed after 38 s (dotted line in Figure 1a). Interference fringes, due to the solvent evaporation, are observed in the first stage and disappear with completion of the process; throughout this stage the film shows a continuous decrease in thickness, as revealed by the increasing distance between the maxima of two adjacent interference fringes. There are basically two regions of interest, the 2700–3700 cm^{-1} region, with the

OH stretching modes, and the 900–1700 cm^{-1} region, with the Si–OH band (around 950 cm^{-1}), the overlapped modes due to EtOH, Si–O–Si stretching, and Si–OR around 1100 cm^{-1} , and the bands due to ethanol and water around 1470 and at 1640 cm^{-1} , respectively.¹⁷

The second stage, which starts after an intermediate stage of few seconds, is characterized by the polycondensation reactions of silica. The increase in intensity of the band around 1100 cm^{-1} (ν_{as} , Si–O–Si) is an indication that the polycondensation reactions are forming a growing silica network. These reactions produce water that again enriches the film; an increase in the intensity of water vibrational bands (1640 and 3300 cm^{-1}) is observed together with the appearance of an intense Si–OH band. This last phenomenon seems contradictory, because condensation leads to the formation of siloxane bonds, Si–O–Si, at the cost of silanols, Si–OH. It can be, however, explained by the fact that even during condensation the hydrolysis can happen to a quite large extent. On the other hand, the formation of silanols can also be a source of water adsorption from the external environment because the film also becomes more hydrophilic, increasing the water adsorption tendency. In a previous paper,^{10a} however, we have performed IR in situ experiments on films prepared by methyltriethoxysilane (MTES)

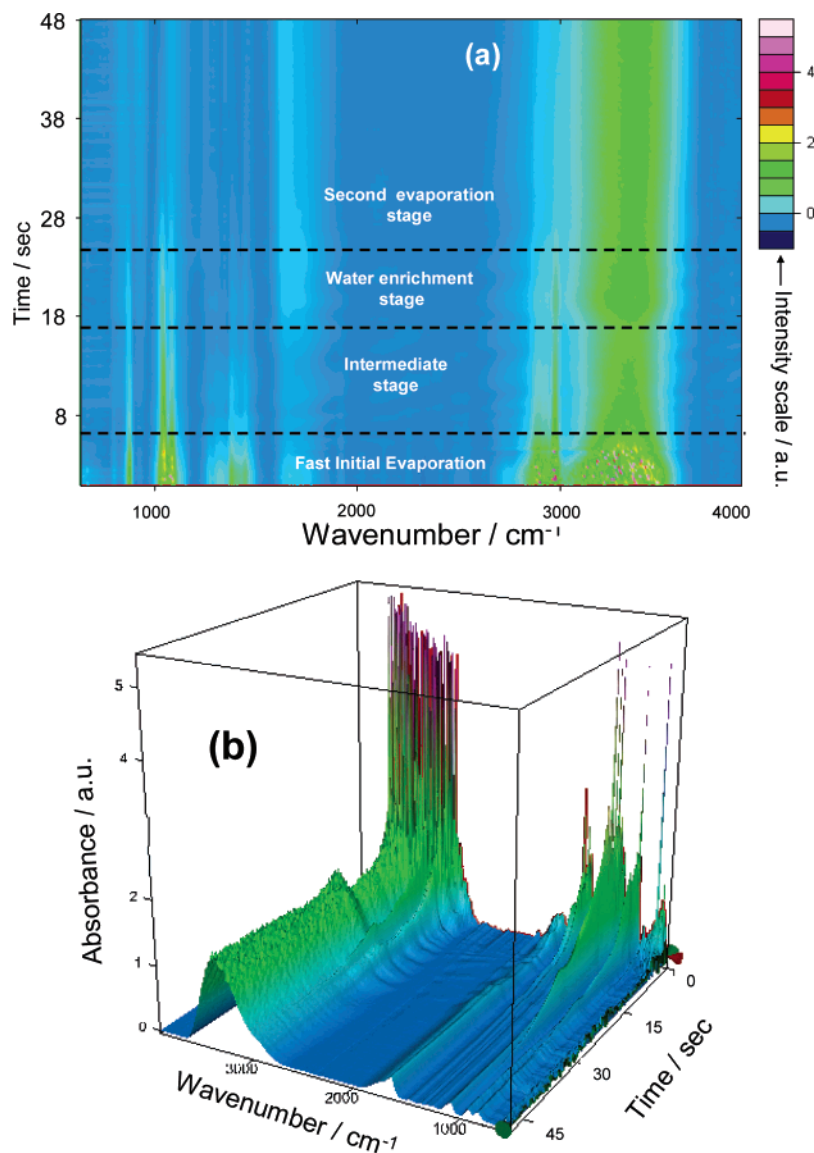


Figure 2. Three-dimensional FTIR images (a and b) obtained during the deposition by casting of a self-assembling titania film. The images are recorded by rapid scan time-resolved method.

or tetraethoxysilane. The water evaporation stage is well observed even in the MTES-based films, whose hydrophobicity due to the presence of methyl groups should hinder or reduce the water absorption from the external environment. The phenomenon is instead again clearly observed even in the presence of methyl groups in the film, and this is a good indication that water released during the condensation reactions is mainly responsible for the water enrichment stage in the silica films.

Together with the increase of the signal of water, after the beginning of polycondensation, an increase in intensity of the C–H stretching band ($2700\text{--}2900\text{ cm}^{-1}$) is observed. This is, however, produced by a not perfect correction of the time-dependent thickness effect, more than by a true chemical process associated with the film formation. While, in fact, in the $800\text{--}1400\text{ cm}^{-1}$ region baseline correction with thickness change is reliable because of the relatively sharp bands involved, in the $2700\text{--}3500\text{ cm}^{-1}$ interval this is more critical because of the presence of the very wide band due to O–H stretching that overlaps the C–H stretching region (see an example of correction effects in the Supporting Information).

It is also interesting to observe the different evolution with time of solvent evaporation and polycondensation. Evaporation

appears as a slow, continuous process, while the abrupt increase in the signal intensity after the first stage shows that polycondensation is a much faster process (Figures 1b and 2b).

Titania Films. We have also applied the RSTR technique to titania mesoporous films. This material has been carefully characterized *in situ* by Crepaldi et al.;¹⁶ they observed that the very low pH of the precursor sol produces a large hydrolysis but a small condensation with the formation of small oligomeric Ti–oxo species. During the evaporation process, different stages were identified by *in situ* 2D small-angle X-ray scattering (SAXS) and interferometry. Some differences between titania and silica films should be expected due to the different reactivities of silica and titania species.

In the case of titania, the analysis is easier because the region around $1000\text{--}1250\text{ cm}^{-1}$ will be free from the mode of silica stretching, and a better visualization of the processes can be expected (Figure 2). The ethanol signals (1275 , 1088 , 1050 , and 881 cm^{-1}) decrease in intensity with time, indicating the continuous advancement of the evaporation process. On the other hand, the evolution of the titania spectra in the $2700\text{--}3700\text{ cm}^{-1}$ interval shows a behavior that is very similar to that of silica. After few seconds from the end of the first initial evaporation, an increase in the OH stretching signal is again

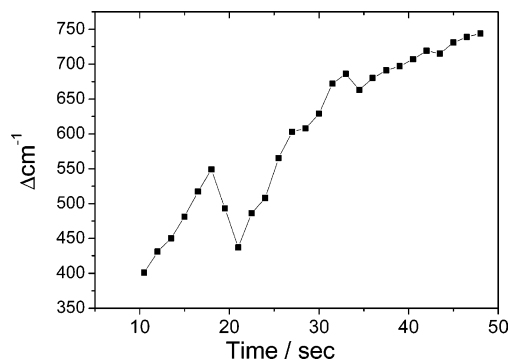


Figure 3. Change of the distance between two adjacent maxima of interference in the 4000–6000 cm^{-1} region, as a function of deposition time. The line is a guide for the eye.

observed. We compared the RSTR results of silica and titania, and the overall deposition process was divided into the following different stages: (a) a fast initial evaporation (FIE); (b) an intermediate stage (IS), which is a stationary stage between the end of solvent evaporation and the beginning of polycondensation; (c) a water enrichment stage (WES), during which the film is enriched in water because of the polycondensation reactions; and (d) a second evaporation stage (SES), the final step with the completion of the polycondensation reactions and the final evaporation of solvent (even if not all the water is evaporated from the film after this step).

We have interpreted the increase in the water content during silica film deposition, which happens only after alcohol evaporation and an intermediate stationary stage, as an indication of the polycondensation reaction (water is released by the classic sol–gel reaction of the alkoxides) and formation of an interconnected oxide network. This is confirmed by the analysis of the single spectra that shows the formation of the silica stretching band exactly in correspondence with the time revealed by RSTR measurements.¹⁰ In the case of titania, however, the water enrichment phase is more difficult to explain. The increase in water can be, in fact, due to some polycondensation reactions of titania but also to water absorption from the external environment, as suggested by Crepaldi et al.¹⁶ The condensation of titania should be, in general, largely hindered in TiCl_4 derived systems, because the HCl generated in situ is retained in solution well beyond the water evaporation and Ti–O–Ti condensation results unlikely in such acidic medium. Absorption of water from the external environment remains, therefore, the most plausible cause of the water enrichment in titania films.

Figure 3 shows the change in the distance between two adjacent interference maxima, which appears in the 4000–6000 cm^{-1} interval, as a function of time, for titania films. The continuous increase of the curve, which is related to the film thickness decrease and the refractive index, shows a discontinuity in correspondence with the WES time. This effect can be produced by a small transient increase in film thickness due to water absorption from the external environment and is good support for the explanation of the water enrichment stage in titania films.

Conclusions

The in situ FTIR spectroscopy through rapid scan time-resolved measurements has been shown to be a very powerful tool to investigate the reactions in thin films during self-assembly. The technique that we have proposed can be also extended in general to the study of deposition of films from liquid phases, such as sol–gel films, and can visualize in a simple and direct way the different processes and their relative

kinetics. Using this technique, four different stages during film casting of self-assembling films have been observed, whose kinetics can be easily measured.

Acknowledgment. Prof. Clement Sanchez of University Paris VI and Dr. Galo Soler-Illia of CNEA, Argentina, are acknowledged for helpful discussions and suggestions. FIRB Italian projects are acknowledged for financial support (FIRB contract RBNE01P4JF).

Supporting Information Available: Reference FTIR absorption spectra of liquid films of ethanol, tetraethoxysilane, and Pluronic F127. Comparison of the RSTR spectra of titania films before and after the baseline correction. This material is available free of charge via the Internet at <http://pubs.acs.org>.

References and Notes

- (1) (a) Brinker, C. J.; Lu, Y.; Sellinger, A.; Fan, H. *Adv. Mater.* **1999**, *11*, 579. (b) Antonietti, M.; Ozin, G. A. *Chem. Eur. J.* **2004**, *10*, 28. (c) Grosso, D.; Cagnol, F.; Soler-Illia, G. J. D. A.; Crepaldi, E. L.; Amenitsch, H.; Brunet-Bruneau, A.; Bourgeois, A.; Sanchez, C. *Adv. Funct. Mater.* **2004**, *14*, 309.
- (2) (a) Soler-Illia, G. J. D. A.; Sanchez, C.; Lebeau, B.; Patarin, J. *Chem. Rev.* **2002**, *102*, 4093. (b) Soler-Illia, G. J. D. A.; Crepaldi, E. L.; Grosso, D.; Sanchez, C. *Curr. Opin. Colloid Interface Sci.* **2003**, *8*, 109.
- (3) (a) Antonietti, M.; Ozin, G. A. *Chem. Eur. J.* **2004**, *10*, 28. (b) Soler-Illia, G.; Innocenzi, P. *Chem. Eur. J.*, in press.
- (4) Huo, Q.; Margolese, D. I.; Ciesla, U.; Demuth, D. G.; Feng, P.; Gier, T. E.; Sieger, P.; Firouzi, A.; Chmelka, B. F.; Schüth, F.; Stucky, G. D. *Chem. Mater.* **1994**, *6*, 1176.
- (5) (a) Klotz, M.; Albouy, P. A.; Ayrat, A.; Menager, C.; Grosso, D.; Van der Lee, A.; Cabuil, V.; Babonneau, F.; Guizard, C. *Chem. Mater.* **2000**, *12*, 1721. (b) Grosso, D.; Balkenende, A. R.; Albouy, P. A.; Ayrat, A.; Amenitsch, H.; Babonneau, F. *Chem. Mater.* **2001**, *13*, 1848.
- (6) (a) Flodstrom, K.; Teixeira, C. V.; Amenitsch, H.; Alfreddsson, V.; Linden, M. *Langmuir* **2004**, *20*, 4885.
- (7) Doshi, D. A.; Gibaud, A.; Liu, N.; Sturmayer, D.; Malanoski, A. P.; Dunphy, D. R.; Chen, H.; Narayan, S.; MacPhee, A.; Wang, J.; Reed, S. T.; Hurd, A. J.; van Swol, F.; Brinker, C. J. *J. Phys. Chem. B* **2003**, *107*, 7683.
- (8) Gibaud, A.; Grosso, D.; Smarsly, B.; Baptiste, A.; Bardeau, J. F.; Babonneau, F.; Doshi, D. A.; Chen, Z.; Brinker, C. J.; Sanchez, C. *J. Phys. Chem. B* **2003**, *107*, 6114.
- (9) Doshi, D. A.; Gibaud, A.; Goletto, V.; Lu, M.; Gerung, H.; Ocko, B.; Han, S. M.; Brinker, C. J. *J. Am. Chem. Soc.* **2003**, *125*, 11646.
- (10) (a) Innocenzi, P.; Malfatti, L.; Kidchob, T.; Falcaro, P.; Cestelli Guidi, M.; Piccinini, M.; Marcelli, A. *Chem. Commun.* **2005**, 2384. (b) Falcaro, P.; Costacurta, S.; Mattei, G.; Amenitsch, H.; Marcelli, A.; Cestelli Guidi, M.; Piccinini, M.; Nucara, A.; Malfatti, L.; Kidchob, T.; Innocenzi, P. *J. Am. Chem. Soc.* **2005**, *127*, 3838.
- (11) Wetzel, D. L. *Vib. Spectrosc.* **2002**, *29*, 291.
- (12) Rapid scan and step scans are two different techniques that can be used to record real time-resolved infrared spectra. In the rapid scan technique, the time-dependent evolution of the infrared active species is observed by recording the spectra in sequence. In this acquisition mode, the time resolution is limited to about 20 ms because of the scanning speed of the moving mirror. In the step-scan mode, instead, the position of the moving mirror is fixed at a particular position, and a complete time run is recorded at this particular mirror position. This procedure is repeated at all other mirror positions, and a 3D representation of the temporal evolution of the entire interferogram is obtained by combining the respective time traces. Fourier transformation yields the corresponding 3D representation of the time evolution of the IR difference spectra.
- (13) Innocenzi, P.; Falcaro, P.; Grosso, D.; Babonneau, F. *J. Phys. Chem. B* **2003**, *107*, 4711.
- (14) X-ray diffraction and SAXS analysis performed on films produced in the same conditions showed *Fmmm* orthorhombic symmetry in the case of silica films and *Im3m* symmetry for titania (see ref 15).
- (15) (a) Malfatti, L.; Falcaro, P.; Amenitsch, H.; Caramori, S.; Argazzi, R.; Bignozzi, C. A.; Enzo, S.; Maggini, M.; Innocenzi, P. *Microporous Mesoporous Mater.* **2006**, *88*, 304. (b) Innocenzi, P.; Malfatti, L.; Kidchob, T.; Falcaro, P.; Costacurta, S.; Guglielmi, M.; Mattei, G.; Amenitsch, H. *J. Synchrotron Radiat.* **2005**, *12*, 734. (c) Falcaro, P.; Grosso, D.; Amenitsch, H.; Innocenzi, P. *J. Phys. Chem. B* **2004**, *108*, 10942.
- (16) Crepaldi, L.; Soler-Illia, G.; Grosso, D.; Cagnol, F.; Ribot, F.; Sanchez, C. *J. Am. Chem. Soc.* **2003**, *125*, 9770.
- (17) For a full attribution of the different vibrational modes see: Innocenzi, P. *J. Non-Cryst. Solids* **2003**, *316*, 309 and references therein.